Engineered Science

RESEARCH PAPER View Article Online

High-performance Engineered Conducting Polymer Film towards Antimicrobial/Anticorrosion Applications

Amit Nautiyal,[1†] Mingyu Qiao,[2†] Tian Ren,[2] Tung-Shi Huang,[2*] Xinyu Zhang,[1*] Jonathan Cook,[1] Michael J. Bozack[3] and Ramsis Farag[4,5]

The goal of this study was to develop a multifunctional coating material that possessed both electrical and antimicrobial properties. Polypyrrole (PPy) has proved to be transformed into *N*-halamine after its treatment with chlorine bleach. This PPy based *N*-halamine was tested to have superior antimicrobial efficacy. Its coating inactivated more than 6 log CFU of both *Staphylococcus aureus* and *Escherichia coli* O157:H7 within one min of contact time. The stability of PPy based *N*-halamine was excellent, maintaining 50% of functional groups after a week storage under fluorescent light. PPy *N*-halamine coating was successfully synthesized by chlorination of electrodeposited PPy coating on the surface of stainless steel. This PPy *N*-halamine coating on stainless steel inactivated 6 log CFU of *S. aureus* within 60s of contact and the antimicrobial activity remained unchanged after a "recharge" cycle. In addition, the PPy *N*-halamine coating significantly enhanced its the anticorrosion functionality by anodically shifting the corrosion potential. This method of preparing antimicrobial/anticorrosion coating is facile, green and highly effective. The produced PPy *N*-halamine showed great potential to be applied as multifunctional coating for protecting steels in harsh environments.

Keywords: *N*-halamines; Conducting polymer; Antimicrobial; Anticorrosion; Coating

Received 20 September 2018**, Accepted** 24 October 2018

DOI: 10.30919/es8d776

1.Introduction

Stainless steel is widely used in the food industry for equipment fabrication such as pipework, tanks, conveyor belts, worktables, machinery parts, etc.[1] However, previous research has shown that stainless steel is prone to harboring pathogenic microorganisms that form biofilms, making it vulnerable as a source for microbial cross-contamination.[2–5] Each year in the United States, 48 million people get sick with 3,000 deaths from foodborne illnesses, with an estimated economic loss of $15.6 billion.[6,7] Foodborne pathogens from food contact surfaces, including stainless steel, can contribute as one of the major source of infection.[8,9] In recent years, developing non-migrate antimicrobial coatings for stainless steel by exploiting advanced materials is a promising solution to tackle microbial cross-contamination problems.[10–14] From all the explored antimicrobial agents, *N*-halamines showed a great potential for applications in the food industry. This is due to their superior antimicrobial efficacy against a broad spectrum of microorganisms, low-toxicity, good stability and low cost.[15–17]

N-halamines are defined as a group of compounds containing one or more nitrogen-halogen bonds that are transformed from nitrogen-hydrogen bonds in groups of imide, amide or amine.[18] The antimicrobial activity of *N*-halamines is contributed from the oxidation state of halide atoms in nitrogen-halogen bonds.[19] An important feature that makes *N*-halamines distinct from other existing biocides is that the antimicrobial activity can be recovered after halide atoms are consumed by treating them with halogenation agents such as chlorine bleach. This "recharging" procedure can be easily incorporated into current sanitation practices applied in the food industry. This makes *N*-halamines an attractive antimicrobial technology for the food industry. Recent reviews and research articles intensively highlighted the great potential of applying *N*-halamine polymers for equipment coatings or packaging in the food industry.[20–25] Some research involved *N*-halamine polymers grafted onto the surfaces of stainless steel. However, to maintain *N*-halamine antimicrobial functional groups (e.g. >N-Cl), chlorine bleach is needed to repeatedly treat the coatings, which may corrode stainless steel.

The corrosion of stainless steel is a serious concern in various industrial application including food industry. The higher grades of stainless steel with better anti-corrosion properties (e.g. 304 and 316 types) are widely used for food equipment fabrication. However, the extended exposure to corrosive agents such as chloride in processing or cleaning agents, chlorine and oxidizing sanitizers, and even food components (e.g. meat/blood) etc., accelerate the steel degradation. These stringent food processing environments make high-grade stainless steel more vulnerable to corrosion. Microbial biofilms also attacks the surface of the stainless steel through excreting oxidative or corrosive metabolites.[26–28] All these factors combined accelerates the corrosion process of stainless steel and cause enormous economic loss to the food industry. Most commonly used strategy to

[1]*Department of Chemical Engineering, Auburn University, Auburn, AL 36849, USA*
[2]*Department of Poultry Science, Auburn University, Auburn, AL 36849, USA*
[3]*Department of Physics, Auburn University, Auburn, AL 36849, USA*
[4]*Center for Polymer and Advanced Composites, Auburn University, Auburn, AL 36849, USA*
[5]*Textile Engineering Department, Mansoura University, Egypt*
[†]*Authors contribute equally for this work*
***E-mail:** huangtu@auburn.edu ; xzz0004@auburn.edu*

protect stainless steel from corrosion is organic coating. The surface is coated with various organic coating including epoxy, acrylic based paints. In addition, electroactive conducting polymers such as polypyrrole, polyaniline etc., are class of materials that are widely used in variety of application areas such as energy storage, catalyst, biosensor etc. in various different morphologies.[29–31] Besides, they are the best candidates for anticorrosive materials, due to their electrical conductivity and their ease of synthesis, both chemically and electrochemically. The electrochemical deposition is the most efficient way to synthesize conducting polymer coatings due to their limited processability issues.[32–35] Compared with other anticorrosion technologies on stainless steel, the synthesis and coating procedures for conducting polymers are fast, simple and green. Conducting polymers, such as polypyrrole, have been reported to be safe for biomedical applications.[36] This is an important criterion for applications of conducting polymer coatings in food contact materials. Previously, within our group, polypyrrole (PPy) has been successfully synthesized on the surface of carbon steel and showed excellent adhesion. In addition to anticorrosive coating, PPy displayed certain biocidal activities.[37] We aim to further improve the antimicrobial properties of conducting polymer coating through *N*-halamine transformation.

In this study, we developed conducting polymer based *N*-halamine coating material to prevent microbial contamination and corrosion of stainless steel with single layer of the coating. Polypyrrole (PPy) being one of the most studied nitrogen based conductive polymers was transformed into *N*-halamines by chlorine bleach treatment in the study and mechanism was illustrated. The antimicrobial activity and stability of transformed coating was also investigated. Moreover, a potential application of our conducting polymer-based *N*-halamine as an antimicrobial/anticorrosion coating on stainless steel was illustrated in this study.

2.Material and methods

2.1.Materials

Pyrrole, platinum (Pt) gauze (100 mesh, 99.9 % metal basis), sodium thiosulfate, and ammonium persulfate were purchased from Alfa Aesar (Heysham, England). Sodium dodecylbenzene sulfonate (SDBS) was obtained from Spectrum Chemicals (New Brunswick, NJ). Potassium iodide was purchased from Fisher Scientific (Fair Lawn, NJ). House bleach was purchased from Walmart (Great Value™). Stainless steel (316 L 24 G, 0.6 mm of thickness) was supplied by Stainless Supply Inc (Monroe, NC). All chemicals were used as received. *Staphylococcus aureus* (ATCC 6538) and *Escherichia coli* O157:H7 (ATCC 43895) were obtained from American Type Culture Collection (ATCC, Rockville, MD).

2.2. Preparation of PPy coating on tape and chlorination

Ppy was synthesized by a chemical oxidative polymerization method following reported procedure.[38] Briefly, 1 mL of pyrrole was added to 60 mL of 1M HCl and stirred for 10 min. After stirring, 1.15 g of ammonium persulfate (APS) was added into the solution. The change of the color from yellowish brown to black is the indication of PPy formation. The solution was then rinsed with copious amount of water followed by filtration and vacuum drying at 60 °C for overnight to obtain black dry PPy granules. The dried PPy were coated onto 3M™ 600 Scotch Transparent Tape (2×2 cm) and pressed to obtain a compact and evenly distributed PPy coating on the surface. The PPy-coated tape films (Tape-PPy) were treated with different concentrations of bleach solutions (0.5, 1, and 5 %) with different treatment times (5, 10, and 30 min) to find out the optimal chlorination condition. After chlorination, the tape films were washed thoroughly with deionized water and dried in a vacuum oven overnight to remove any free chlorine residuals. The uncoated tape film was treated with the same procedure to serve as chlorination control. The formation of nitrogen-halogen bonds (>N-Cl) from nitrogen-hydrogen bonds (>N-H) in PPy was confirmed by X-ray photoelectron spectroscopy (XPS) using a load-locked Kratos XSAM800 surface analysis system equipped with a hemispherical energy analyzer, and Fourier transform infrared spectroscopy (FT-IR) using a Thermo Scientific Nicolet™ 6700 Spectrometer.

2.3.Determination of chlorine content and stability test

The oxidative chlorine contents of chlorinated PPy-coated tape films (Tape-PPy-Cl) were determined using an iodometric/thiosulfate titration method.[39] Briefly, a piece of Tape-PPy-Cl film was put into a flask containing 20 mL of water, 10 µL of 0.1 N acetic acid and 0.2 g of potassium iodine and stirred at room temperature for 20 min. Then, 0.5% starch solution to above solution and titrated by 0.001 N sodium thiosulfate. The active chlorine content was calculated using the following formula: $[Cl^+]$ ($\mu g/cm^2$) = $(N \times V \times 35.5)/2A$, where N and V are the normality ($equiv \cdot L^{-1}$) and volume (L) of the titrant sodium thiosulfate and A is the total surface area of titrated sample (cm^2). The stability of PPy *N*-halamine under three different conditions (dark, fluorescent light and Ultraviolet) was determined based on chlorine content measured by the titration method. After a certain period of storage time, oxidative chlorine content of three Tape-PPy-Cl films from each storage condition was measured.

2.4.Antimicrobial efficacy test with PPy *N*-halamine coated tape

The antimicrobial efficacy of PPy *N*-halamine coated tape films was determined using a "sandwich" method as described previously.[39] A gram-negative bacterium of *E. coli* O157:H7 and a gram-positive bacterium of *S. aureus* were used in this study. A single colony of each bacteria was transferred into 15 mL of Trypticase soy broth (Becton and Dickinson Co., MD) and incubated at 37 °C for 16 h. The culture was washed twice with Butterfield's phosphate buffer (BPB) through centrifugation and was re-suspended in the BPB buffer. Bacterial population was estimated by the absorbance at $O.D._{640\ nm}$ and the inoculum with the designated population was prepared. An aliquot of 25 µL of the inoculum was added into the center of the square film, and a second identical film was placed on the sample to ensure complete contact with inoculated bacteria. A sterile weight was placed on the top to ensure complete contact with inoculated bacteria. At the contact times of 1, 5, and 10 min, the films were transferred into $Na_2S_2O_3$ solution (0.05 N) and vortexed vigorously to quench any oxidative chlorine residuals and to detach survived bacteria from the sample. Ten-fold serial dilutions were made for all samples and each dilution was plated on Trypticase soy agar plates (Becton and Dickinson Co., MD). The plates were incubated at 37 °C for 48 h and bacterial colonies were enumerated and recorded for antimicrobial efficacy analysis.

2.5.Preparation of PPy *N*-halamine-coated stainless steel

Ppy was coated onto the surface of stainless steel (SS) using an electrochemical method (Scheme 1). SS plate was cut into coupons (1.5×1.5 cm) and was cold mounted into acrylic resin so that only

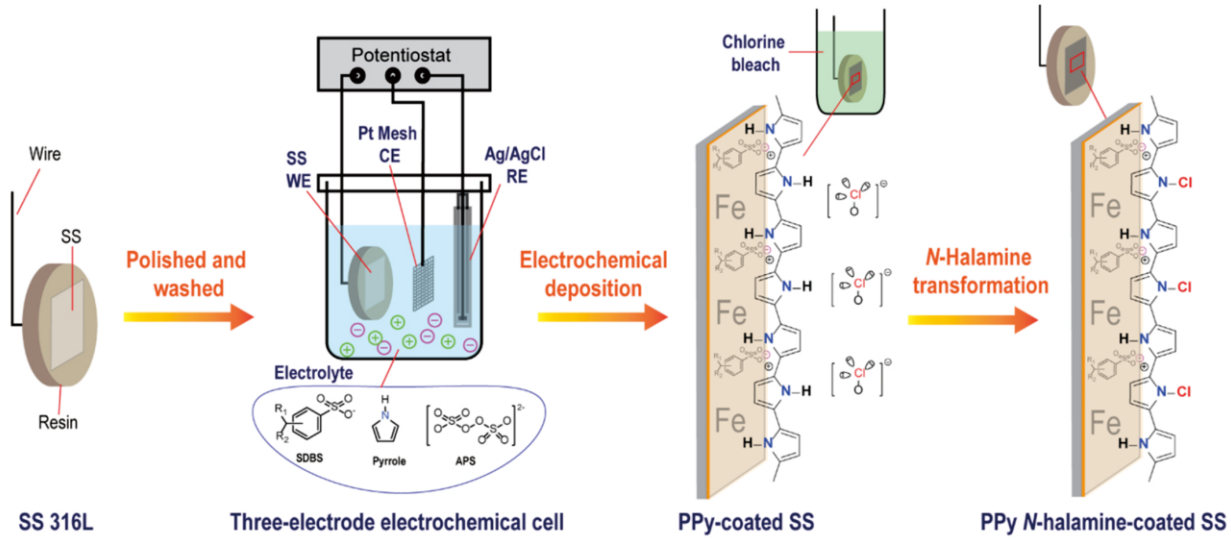

Scheme 1. Illustration of the preparation of PPy *N*-halamine-coated stainless steel.

one surface was exposed to the electrolyte. After drying overnight, the embedded SS sample was polished with 800, 1000 and 1200 grit size sandpapers (3M™ Imperial Wetordry™) and washed thoroughly with deionized water. PPy coating was electrochemically deposited from an electrolyte solution containing the pyrrole (0.1 M) and sodium dodecylbenzene sulfonates (SDBS, 25 mM). The electrochemical cell used was a single compartment system with three electrodes: SS plate served as a working electrode, Pt mesh as a counter electrode and Silver/Silver chloride/KCl (3 M) (Ag/Ag^{+}, E° = +205 mV vs. SHE) and Mercury/Mercury Sulfate/K_2SO_4 (saturated) (MSE, E° = +650 mV vs. SHE) were used as reference electrodes. Potentiostatic deposition was carried out on CH Instrument potentiostat (CHI 601D) with Electrochemical Analyzer software (Version 15.03) by applying 0.8 V/MSE for 5 min. The formation of a black thin film on the surface of SS plate indicated the successful deposition of PPy coating. For *N*-halamine transformation, PPy-coated SS samples were immersed in 1 % chlorine bleach (pH 7.0/HCl, $[Cl^{+}]$ = 414±8 ppm) for 10 min, washed thoroughly with deionized water and dried overnight in a vacuum oven.

2.6.Characterization of PPy *N*-halamine-coated stainless steel

Surface morphology of the coatings was analyzed using a Scanning Electron Microscopy (SEM) on JOEL JSM-7000F at 20 keV with 10 mm working distance. Surface energy of the coating was measured using a ramé-hart Standard Contact Angle Goniometer Model 200 (ramé-hart Inc., Mountain Lakes, NJ) equipped with DROP image software. The water contact angles were measured using the sessile drop method and three independent measurements were performed for each type of sample. The formation of nitrogen-chlorine bond from nitrogen-hydrogen bond was confirmed with X-ray Photoelectron Spectroscopy (XPS) through analyzing the presence of chlorine element. The thickness of the coating d (cm) was calculated using equations (i) and (ii):[40]

$$d = \frac{m}{2\rho} \quad \text{(i)}$$

$$m = \frac{Q\,(M_m + \gamma\, M_d)}{F(2+\gamma)A} \quad \text{(ii)}$$

where, Q was the total Faradic charge consumed in the electropolymerization (1.86 C), M_m was the molar mass of the monomer (pyrrole, 67.09 g/mol), M_d was the molar mass of the dopant (dodecylbenzene sulfonate, 348.48 g/mol), γ was the doping density of polypyrrole (0.33), F was Faradic constant (96,485 C/mol), A was the surface area (cm^2), and ρ was density of the polymer (1.48 g/cm^3).

2.7.Antimicrobial efficacy test with PPy *N*-halamine coated stainless steel

Antimicrobial efficacy was determined using the same "sandwich" method as mentioned previously in this study. The PPy-coated and PPy *N*-halamine-coated SS samples were autoclaved at 121 °C for 45 min and dried before use. An aliquot of 10 µL *S. aureus* was inoculated and contact times of 1 and 5 min were performed. After antimicrobial test (experiment 1), all tested samples were recycled and autoclaved. Then samples were treated with $Na_2S_2O_3$ to reduce the >N-Cl in PPy *N*-halamine to >N-H. This process of quenching chlorine from the PPy *N*-halamine coated stainless steel was called "discharge". The "discharged" PPy coated SS was "recharged" back to PPy *N*-halamine coated SS through rechlorinating in 1% bleach for 10 min. These "recharged" PPy *N*-halamine coated SS were used for the second antimicrobial efficacy test (experiment 2) following the same procedures as in experiment 1.

2.8.Anticorrosion test

The PPy *N*-halamine coated SS samples were evaluated for the ability to protect SS from corrosion by immersing in 3.5 % NaCl. The corrosion potential was measured using linear sweep voltammetry (LSV) techniques scanning ±150 mV from the open circuit potential (OCP) at a scan rate of 1 mV/s.

2.9.Electrical conductivity measurement

The bulk electrical conductivity of the PPy *N*-halamine coating was measured using a linear four-probe method as previously described.[41] PPy coating and *N*-halamine coating were touched with a linear four probe which was connected to a multifunctional switch/measurement unit (Agilent 34980A) and specific resistivity was recorded. Conductivity of the deposited coatings σ (S/cm) was calculated using the equation (iii) and (iv):

$$\rho = 4.532 \times t \times R \quad \text{(iii)}$$

$$\sigma = \frac{1}{\rho} \quad \text{(iv)}$$

where, t was the thickness of the coating (cm) and R was the resistance (Ω).

3. Results and discussion

Ppy was successfully coated on the surface of the tape and the polymer content was calculated at 0.3 mg/cm^2. After treated with 5% bleach for 5 min, a yellowish color was observed. With the increasing treatment time and bleach concentration, more PPy was detached from the tape surface (Fig. 2a). This could be explained by the attacking of NaClO in bleach solution to adhesive polymers on the tape. Within the treatment time of 5 min, a higher concentration of bleach resulted in higher content of oxidative chlorines on surface of PPy coated tape (Fig. 2b). At lower bleach concentrations (1 and 0.2 %), longer treatment time resulted in higher oxidative chlorine content. When the bleach concentration reached 5 %, the chlorine content was lower with longer treatment time due to the detachment of PPy polymers from the tape surface. However, the treatment of 5 % bleach for 5 min showed the highest oxidative chlorine content on the surfaces ([Cl^+] = 6.7 μg/cm^2). Therefore, this condition was used to chlorinate samples for the following experiments.

The presence of oxidative chlorine on chlorinated PPy coating could be explained by the hypothesis that part of the nitrogen-hydrogen bonds (>N-H) in PPy structure were transformed into nitrogen-chlorine bonds (>N-Cl) through reacting with NaClO and became *N*-halamine polymers (Fig. 3). The conducting form of PPy with positive charge created empty orbitals in the nitrogen atom of the backbone (approximately 33.3 %), therefore the attack from electron-rich ClO^- was favored and >N-Cl bond was formed. This hypothesis was confirmed based on the results of chlorine titration and spectroscopy. The iodometric reaction ($2I^- + Cl^+ \leftrightarrow I_2 + Cl^-$) indicated that the chlorine element in chlorinated PPy coating was in the oxidative form. After chlorination treatment, the peak of chlorine element was observed on the XPS spectra of PPy coated tape (Fig. 4). In the FT-IR spectra (Fig. 5), the band located at 1539.7 cm^{-1} was attributed to the C=C/C-C stretching vibration of the PPy chains. [42] After chlorination, the vibrational band shifted to 1548.8 cm^{-1}, due to electron-withdrawing effect of the chlorine atoms in the >N-Cl bond.[43] These strong evidences indicate that >N-Cl was formed in PPy after chlorination. Based on these evidences, it was concluded that PPy can be transformed into *N*-halamines after chlorination. The PPy *N*-halamine was recorded as PPy-Cl in this study.

Ppy coated tape caused 0.93 log CFU reduction of *E. coli* O157:H7 and 1.57 log CFU reduction of *S. aureus* within 10 min of contact (Table 1) and were higher than tape only. This slight increase of antimicrobial activity was due to the weak antimicrobial activity of PPy.44 After being transformed into *N*-halamine, the coated tape killed all inoculated bacteria (both *S. aureus* and *E. coli* O157:H7) within 60s of contact, which antimicrobial activity was highly potent. This significant improvement of antimicrobial activity was contributed from the oxidative chlorines in >N-Cl of PPy based *N*-halamine.

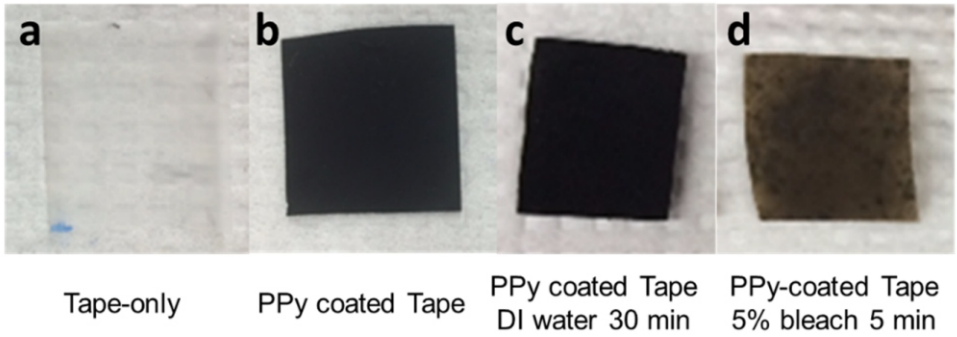

Fig. 1 Appearance of PPy-coated tape films.

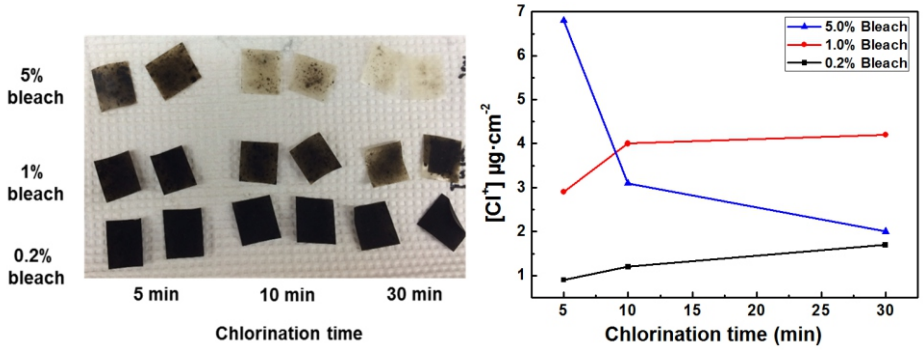

Fig. 2 Appearance (left) and oxidative chlorine content (right) of PPy *N*-halamine coating on tape after different concentrations and times of chlorine bleach treatment.

Table 1. Antibacterial efficacies of PPy *N*-halamine coated tape.[a]

Samples	Contact time	Bacterial reduction (log CFU)	
		E. coli O157:H7	*S. aureus*
Tape -Cl	10 min	0.78	1.00
Tape -PPy	10 min	0.93	1.57
	1 min	6.25 *	6.19 *
Tape -PPy -Cl	5 min	6.25 *	6.19 *
	10 min	6.25 *	6.19 *

[a] Chlorination condition: 5% bleach for 5 min. Inoculum: 6.25 log CFU/sample of *E. coli* O157:H7, 6.19 log CFU/sample of *S. aureus*. * Total killing of inoculated bacteria under detection limit.

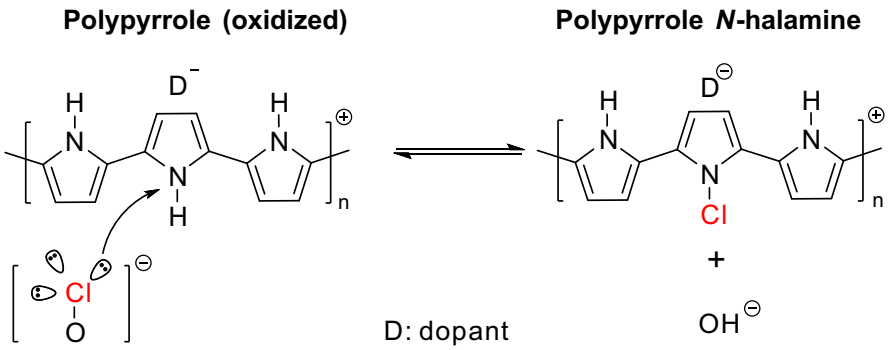

Fig. 3 Mechanism of polyprrole transformed to *N*-halamine by chlorine bleach treatment.

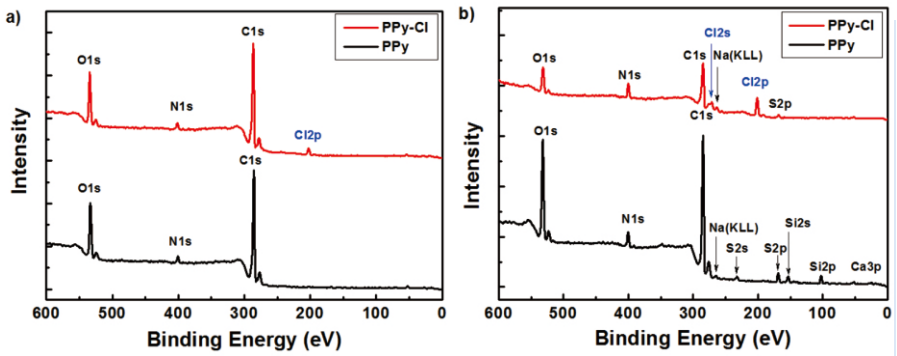

Fig. 4 XPS spectra of PPy and PPy *N*-halamine coated on: a) tape and b) stainless steel.

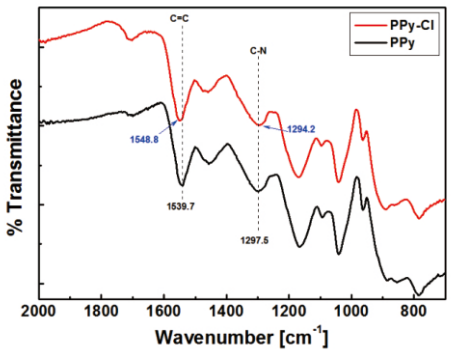

Fig. 5 FT-IR spectra of PPy and PPy *N*-halamine.

N-halamine compounds usually have potent antimicrobial activity based on previous research.[18,19] Compared with all other *N*-halamines found to date, the antimicrobial activity of PPy *N*-halamine was one of the most robust and effective. The superior antimicrobial function of PPy *N*-halamine was ascribed to high density of >N-H bonds in PPy polymers that resulted in the formation of more >N-Cl groups on the surface. These >N-Cl in PPy *N*-halamine is highly active due to the structure of pyrrole (Figure 6). Usually, the biocidal activity of *N*-halamine follows the orders of imide > amide > amine (Fig. 6). To date, cyclic hydantoin based *N*-halamine (Fig. 6) containing both amide and imide groups were found to be the most potent *N*-halamine functional structures and their coating on fabrics could inactivate 100% bacteria within 1-5 min using the same testing procedures reported study.[45] The biocidal activity of PPy *N*-halamine was comparable to the strong *N*-halamine polymers based on the cyclic hydantoin structure. The potent antimicrobial activity in PPy *N*-halamine may be influenced by the adjacent C=C bond as the similar mechanism of adjacent C=O bond in imide and amide *N*-halamines.

Based on previous research, the *N*-halamine bond (>N-Cl) was not stable under UV light. For these *N*-halamines with good antimicrobial activity such as imide and amide, the decrease of stability was often observed.[46] Therefore, the stability of PPy *N*-halamine coating was also investigated in this study (Table 2). The PPy based *N*-halamine lost 58 % of oxidative chlorines on coated surface after storage under UV for 24 h. Under fluorescent light,

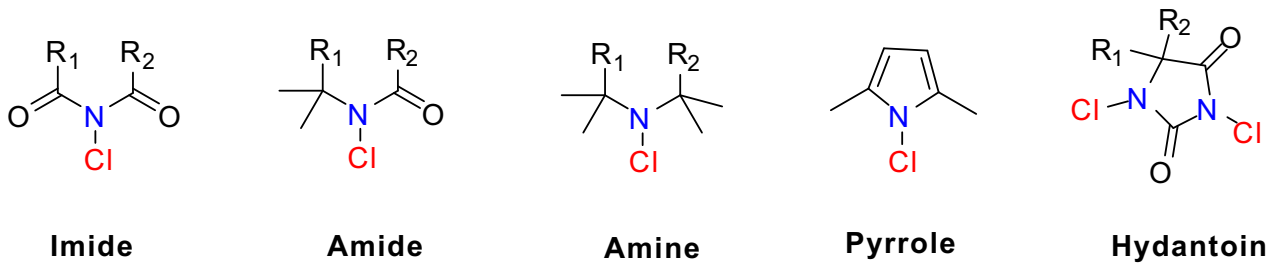

Fig. 6 Molecular structures of various *N*-halamines mentioned in this study.

Table 2. Stability of PPy *N*-halamine coating on tape under different storage conditions.

UV		Fluorescent Light		Dark	
Time (h)	$[Cl^+]$ (μg/cm^2)	Time (d)	$[Cl^+]$ (μg/cm^2)	Time (d)	$[Cl^+]$ (μg/cm^2)
0	5.33	0	5.33	0	5.33
1	4.73	1	4.44	1	5.33
3	3.33	3	2.96	3	4.44
12	3.11	5	2.66	7	2.81
24	2.22	7	2.66	14	1.04

50% percent of oxidative chlorines were lost after storage for one week while in dark condition for two weeks, only 20 % of oxidative chlorine remained on the surface. The stability of *N*-halamine functional group (>N-Cl) in PPy was not as good as cyclic hydantoin based *N*-halamine containing amide group, which retained 67 % of oxidative chlorines after 15 days storage under dark.[47] Usually, sanitation was performed every day in food processing plant, which means the recharge process can be repeated within a day. Therefore, PPy *N*-halamine has sufficient stability for supporting the application as antimicrobial equipment coating in the food processing environment. The stability of *N*-halamine can be further improved through the combination with titanium dioxide (TiO_2), which has been routinely used as an antimicrobial agent on stainless steel surface.

In Fig. 7, a typical chronoamperometry curve was observed during the electrodeposition of polypyrrole on stainless steel surface. Initially, there was a sharp increase in current density indicating the diffusion-controlled pyrrole oxidation and nucleation of radical cation of pyrrole on the steel surface. After nucleation, the current density remained constant corresponding to continuous growth of polypyrrole film on stainless steel.

Ppy was successfully coated on the surface of stainless steel (Fig. 8a) and formed homogenous film (Fig. 8b). After being treated with 1% bleach for 10 min, no damage was observed on the coated surface (Fig. 8c). Therefore, 1 % bleach for 10 min treatment was used to chlorinate the PPy coating on stainless steels and the chlorine content was 2.05±0.15 μg/cm^2. It was also found that there was no damage of the coating after sterilization at 121 °C for 45 min (Fig. 8d).

The antimicrobial activity of PPy *N*-halamine coated stainless steel was tabulated in Table 3. The bare stainless steel caused 0.94 log

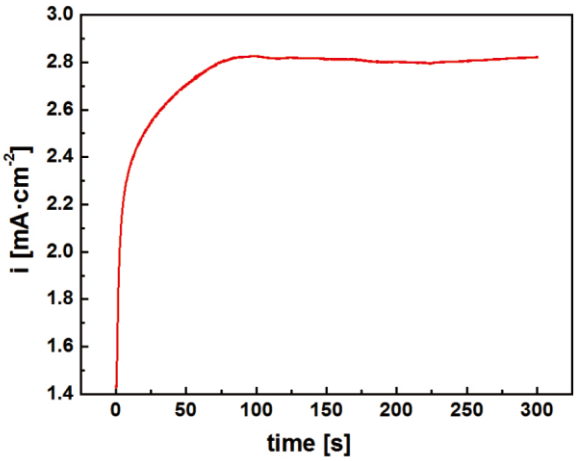

Fig. 7 Chronoamperometry curve of electropolymerization of polypyrrole on stainless steel.

CFU reduction of *S. aureus* after 5 min of contact; however, PPy *N*-halamine coated stainless steel killed all inoculated bacteria (6.29 log CFU) within 60s of contact time. The antimicrobial activity remained unchanged after being rechlorinated for one time, which indicated that the antimicrobial function of PPy *N*-halamine coating could be recharged. It was unexpected that the unchlorinated PPy coating on stainless steel was also able to have a total kill of bacteria (6.29 log CFU reduction) in experiment 1. This may due to the use of dodecylbenzene sulfonate (SDBS) as dopant, which is also a strong antimicrobial agent.[48] From our previous study, SDBS as dopant gave the optimum adhesive and anticorrosion property to PPy coated

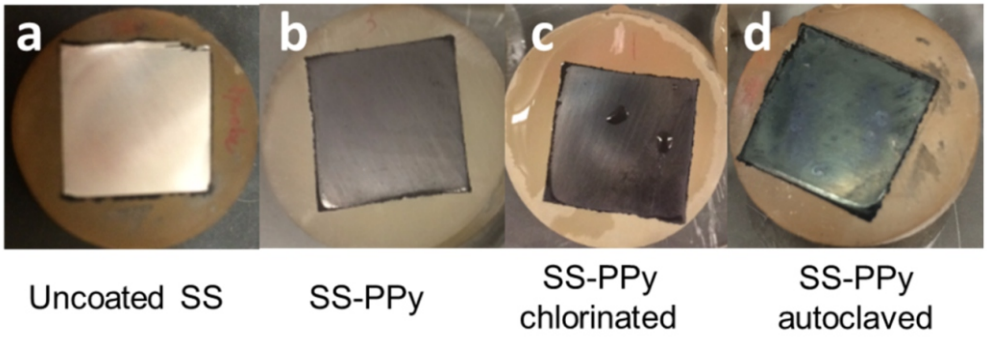

Fig. 8 Appearance of (a) uncoated stainless steel, (b) PPy coated stainless steel, (c) PPy coated stainless steel after chlorination treatment in 1% bleach for 10 min, and (d) PPy coated stainless steel after autoclave at 121 °C for 40 min.

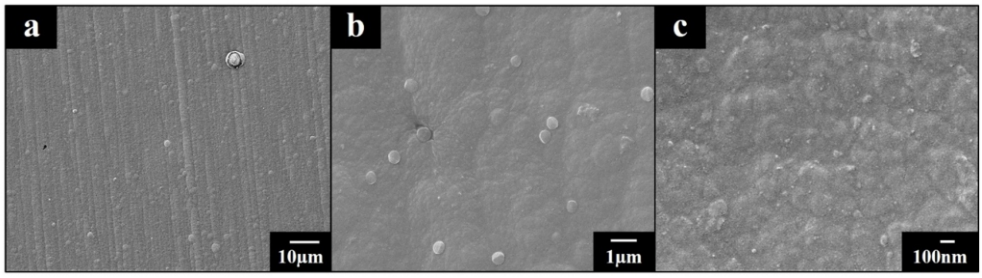

Fig. 9 SEM images of PPy coated stainless steels at different magnifications.

Table 3. Rechargeable antimicrobial function of PPy *N*-halamine coating on stainless steel.[a]

Samples	Contact time	Bacterial reduction (log CFU)	
		Experiment 1	Experiment 2
SS	1 min	0.68	0.81
	5 min	0.94	1.00
SS-PPy	1 min	6.29*	3.89
	5 min	6.29*	4.49
SS-PPy-Cl [a]	1 min	6.29*	6.02*
	5 min	6.29*	6.02*

[a] Chlorination conditions: 1% bleach for 10 min. Experiment 1: first-time chlorination, inoculum 6.29 log CFU/sample of *S. aureus*. Experiment 2: discharged and rechlorinating, inoculum 6.02 log CFU/sample of *S. aureus*.* Total killing of inoculated bacteria under detection limit.

stainless steel.[37] Therefore, the antimicrobial effect of unchlorinated PPy-coated SS was attributed to the synergetic antimicrobial activity of SDBS and PPy. However, the SDBS on the coating surface attached to PPy backbones through ionic attraction, which is easily to be removed after vigorous vortexing in a buffer solution. Therefore, a decrease of antimicrobial activity was observed in experiment 2 with unchlorinated PPy coated stainless steel. The other fact was that, in the previous section (Table 1), when Cl^- was used as the dopant instead of SDBS, the PPy coating on tape caused only one log CFU reduction of bacteria within 10 min of contact. Based on these results, it was confirmed that the potent antimicrobial function of PPy *N*-halamine-coated stainless steel was mainly contributed from *N*-halamine functional groups (>N-Cl). The antimicrobial activity remained unchanged after one cycle of discharge and recharge process, which indicated that the PPy *N*-halamine coating on stainless steel had rechargeable antimicrobial function.

Fig. 10 showed anticorrosive performance of polypyrrole coating and it ennobled the SS surface by shifting its corrosion potential (E_{corr}) from -0.12 to +0.15 V vs Ag/Ag^+. Although there was a slight decrease (30 mV) in corrosion potential after chlorination, the E_{corr} of +0.12 V vs Ag/Ag^+ was still considered good anticorrosion ability. The decrease in corrosion potential is due to the removal of SDBS from PPy that protect the surface synergistically with PPy. SDBS was used as both dopant for the polymer and corrosion inhibitor simultaneously. The

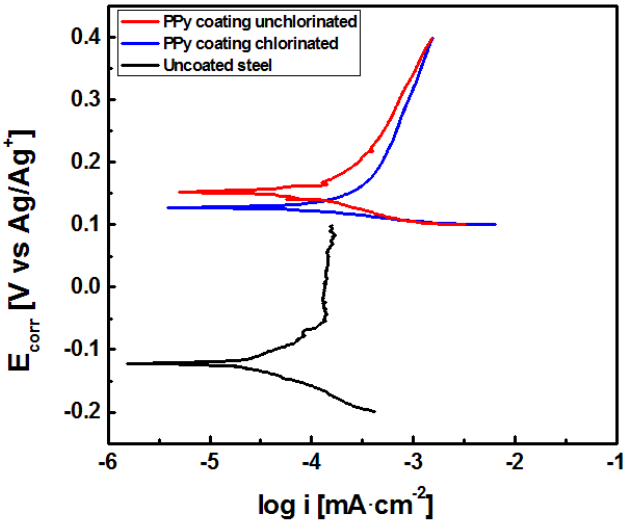

Fig. 10 Polarization curves of polypyrrole (unchlorinated and chlorinated) coated compared with uncoated stainless steel in 3.5% wt. NaCl.

mechanism of corrosion inhibition is that functional groups adsorb on the surface and form aggregates, which contributes to additional protection originally from a single layer of polypyrrole thus enhancing the nobleness of the surface. The resistances were 5 and 200 kΩ for unchlorinated and chlorinated polypyrrole coating, respectively. The conductivity was calculated to be dropped from 1.96 S/cm to 0.049 S/cm, which is still in semiconducting range. The formation of N-Cl bond to a certain extent blocked the electron transfer in the original conducting structure of oxidized PPy; however, this slight decrease in conductivity did not affect the function of PPy conducting polymer as anti-corrosive coating.

4. Conclusions

Ppy conducting polymer was transformed into *N*-halamines after chlorination with bleach. This PPy *N*-halamine had superior antimicrobial activity which inactivated 6 log CFU of both *S. aureus* and *E. coli* O157:H7 within 60s of contact time. The PPy *N*-halamine structure was relative stable under fluorescent light and dark. A thin PPy film was successfully coated onto the surface of stainless steel 316 L through electrochemical deposition. The coating has the potential to withstand aggressive conditions such as high pressure, high temperature, vigorous washing with salt and sanitation solutions, etc. The PPy coating on stainless steel was transformed into *N*-halamine after bleach treatment. This *N*-halamine coated stainless steel inactivated 6 log CFU of *S. aureus* with 60s of contact and the antimicrobial function could be recharged. The PPy *N*-halamine coating significantly improved the corrosion protection of stainless steel. This reported method for preparing antimicrobial/anticorrosion coatings on stainless steel is simple, green and highly effective. It has a great potential to apply as low-cost and high-performance multifunctional coatings for protecting steels used in the food and biomedical industries.

Acknowledgement

This material is based upon work that is supported in part by the Alabama Agricultural Experiment Station. The authors thanked Michelle D. Hayden for reviewing the manuscript.

Notes

The authors declare no competing financial interest.

References

1. R. Schmidt, D. Erickson, S. Sims and P. Wolff, *Food Prot. Trends*, 2012, **32**, 10.
2. A. Kreske, J. Ryu, C. Pettigrew and L. Beuchat, *J. Food Prot.*, 2006, **69**, 2621-2634.
3. R. Chmielewski and J. Frank, *Compr. Rev. Food Sci. Food Saf.*, 2003, **2**, 22-32.
4. J. Brooks and S. Flint, *Int. J. Food Sci. Technol.*, 2008, **43**, 2163-2176.
5. J. Ryu and L. Beuchat, *Am. Soc. Microbiol.*, 2005, **71**, 247-254.
6. E. Scallan, R. Hoekstra, F. Angulo, R. Tauxe, M. Widdowson, S. Roy, J. Jones and P. Griffin, *Emerging Infect. Dis.*, 2011, **17**, 7-15.
7. S. Hoffman, M. Batz and J. Morris, *J. Food Prot.*, 2012, **75**, 1292-1302.
8. A. Lianou and J. Sofos, *J. Food Prot.*, 2007, **70**, 2172-2198.
9. C. Kumar, S. Anand, *Int. J. Food Microbiol.*, 1998, **42**, 9-27.
10. L. Bastarrachea, J. Goddard, *J. Appl. Polym. Sci.*, 2013, **127**, 821-831.
11. C. Falentin-Daudré, E. Faure, T. Svaldo-Lanero, F. Farina, C. Jérôme, C. Van De Weerdt, J. Martial, A. Duwez and C. Detrembleur, *Langmuir*, 2012, **28**, 7233-7241.
12. M. Ignatova, S. Voccia, S. Gabriel, B. Gilbert, D. Cossement, R. Jerome, C. Jerome, *Langmuir* **2009**, *25*, 891-902.
13. S. Jampala, M. Sarmadi, E. Somers, A. Wong and F. Denes, *Langmuir*, 2008, **24**, 8583-8591.
14. A. Madkour, J. Dabkowski, K. Nüsslein and G. Tew, *Langmuir*, 2009, **25**, 1060-1067.
15. L. Bastarrachea, A. Denis-Rohr and J. Goddard, *Annu. Rev. Food Sci. Technol.*, 2015, **6**, 97-118.
16. E. Kenawy, S. Worley and R. Broughton, *Biomacromolecules*, 2007, **8**, 1359-1384.
17. A. Dong, Y. Wang, Y. Gao, T. Gao and G. Gao, *Chem. Rev.*, 2017, **117**, 4806-4862.
18. Z. Chen and Y. Sun, *Ind. Eng. Chem. Res.*, 2006, **45**, 2634-2640.
19. F. Hui and C. Debiemme-Chouvy, *Biomacromolecules*, 2013, **14**, 585-601.
20. M. Qiao, T. Ren, T. Huang, J. Weese, Y. Liu, X. Ren and R. Farag, *RSC Adv.*, 2017, **7**, 1233-1240.
21. L. Bastarrachea and J. Goddard, *J. Agric. Food. Chem.*, 2015, **63**, 4243-4251.
22. L. Bastarrachea, L. Mclandsborough, M. Peleg and J. Goddard, *J. Food Sci.*, 2014, **79**, 887-897.
23. L. Bastarrachea, M. Peleg, L. McLandsborough and J. Goddard, *J. Food Eng.*, 2013, **117**, 52-58.
24. A. Denis-Rohr, L. Bastarrachea and J. Goddard, *Food Bioprod. Process.*, 2015, **96**, 12-19.
25. L. Bastarrachea, S. Dhawan and S. Sablani, *Food Eng. Rev.*, 2011, **3**, 79-93.
26. J. Ibars, D. Moreno and C. Ranninger, *Microbiologia (Madrid, Spain)*, 1992, **8**, 63-75.
27. H. Videla, *Int. Biodeterior. Biodegrad.*, 2001, **48**, 176-201.
28. B. Little and J. Lee, in *Kirk-Othmer Encyclopedia of Chemical Technology*, **2009**, pp. 1–42.
29. M. Schirmeisen and F. Beck, *J. Appl. Electrochem.*, 1989, **19**, 401-409.
30. M. Rizzi, M. Trueba and S. Trasatti, *Synth. Met.*, 2011, **161**, 23-31.
31. L. Zhang, W. Du, A. Nautiyal, Z. Liu and X. Zhang, *Sci. China Mater.*, 2018, **61**, 303-352 .
32. G. Spinks, A. Dominis, G. Wallace and D. Tallman, *J. Solid State Electrochem.*, 2002, **6**, 85-100.

33. D. Tallman, G. Spinks, A. Dominis, G. Wallace, *J. Solid State Electrochem.*, 2002, **6**, 73-84.
34. M. González and S. Saidman, *Prog. Org. Coat.,* 2015, **78**, 21-27.
35. S. Moraes, D. Huerta-Vilca and A. Motheo, *Prog. Org. Coat.*, 2003, **48**, 28-33.
36. X. Wang, X. Gu, C. Yuan, S. Chen, P. Zhang, T. Zhang, J. Yao, F. Chen and G. Chen, *J. Biomed. Mater. Res. Part A*, 2004, **68**, 411-422.
37. A. Nautiyal, M. Qiao, J. Cook, X. Zhang and T. Huang, *Appl. Surf. Sci.*, 2018, **427**, 922-930.
38. S. Poyraz, I. Cerkez, T. Huang, Z. Liu, L. Kang, J. Luo and X. Zhang, *ACS Appl. Mater. Interfaces*, 2014, **6**, 20025-20034.
39. Y. Liu, J. Li, X. Cheng, X. Ren and T. Huang, *J. Mater. Chem. B*, 2015, **3**, 1446-1456.
40. A. Nautiyal and S. Parida, *Prog. Org. Coat.*, 2016, **94**, 28-33.
41. Z. Liu, J. Wang, V. Kushvaha, S. Poyraz, H. Tippur, S. Park, M. Kim, Y. Liu, J. Bar, H. Chen and X. Zhang, *Chem. Commun.*, 2011, **47**, 9912-9914.
42. J. Tabačiarová, M. Mičušík, P. Fedorko and M. Omastová, *Polym. Degrad. Stab.*, 2015, **120**, 392-401.
43. Z. Jiang, B. Demir, R. Broughton, X. Ren, T. Huang and S. Worley, *J. Appl. Polym. Sci.*, 2016, **133**, 26-28.
44. F. Da Silva, J. Queiroz, E. Macedo, A. Fernandes, N. Freire, M. Da Costa, H. De Oliveira, *Mater. Sci. Eng., C*, 2016, **62**, 317-322.
45. H. Kocer, I. Cerkez, S. Worley, R. Broughton and T. Huang, *ACS Appl. Mater. Interfaces*, 2011, **3**, 3189-3194.
46. Y. Liu, J. Li, L. Li, S. McFarland, X. Ren, O. Acevedo and T. S. Huang, *ACS Appl. Mater. Interfaces*, 2016, **8**, 3516-3523.
47. Y. Liu, Q. He, R. Li, D. Huang, X. Ren and T. S. Huang, *Fibers Polym.*, 2016, **17**, 2035-2040.
48. B. Cords, S. Burnett, J. Hilgren, M. Finley and J. Magnuson, in *Antimicrobials in Food*, **2005**, pp. 533–536.